EFECTUL RAPORTULUI APĂ/LIANT ASUPRA PROPRIETĂȚILOR MECANICE DINAMICE ALE UNOR COMPOZITE PE BAZĂ DE CIMENT ARMATE DISPERS CU FIBRE DE PVA

EFFECT OF WATER BINDER RATIO ON DYNAMIC MECHANICAL PROPERTIES OF PVA FIBER REINFORCED CEMENT-BASED COMPOSITE

ZHITAO CHEN, YINGZI YANG*, YAN YAO, YANGCAN WU
School of Civil Engineering, Harbin Institute of Technology, Harbin 150006, China

Quasi-static compressive strength and dynamic impact compressive response of PVA fiber reinforced cement-based composite (PVA-FRCC) with different water binder ratio were studied. The quasi-static compressive strength decreased with increasing water binder ratio. The split Hopkinson pressure bar (SHPB) was used to obtain the dynamic impact compressive response of PVA-FRCC. The results showed that the stress-strain relationship of PVA-FRCC with different water binder ratio performed obvious strain rate effect. The deformation capacity of PVA-FRCC under dynamic load was improved with the increase of water binder ratio. The energy absorption capacity also performed rate dependency; as water binder ratio increase, the energy absorption capacity of PVA-FRCC was weakened.

Au fost studiate rezistențele la compresiune quasi-statică şi la impact dinamic ale unor compozite pe bază de ciment armate dispers cu fibre de PVA (PVA-FRCC). Rezistența la compresiune quasi-statică scade cu creşterea raportului liant apă. Pentru determinarea impactului dinamic asupra rezistenței la compresiune a PVA-FRCC s-a utilizat echipamentul Hopkinson. Rezultatele experimentale au indicat faptul că relațiile efort unitar deformație specifică ale unor compozite pe bază de ciment armate dispers cu fibre (PVA-FRCC) având diferite rapoarte apă/liant sunt influențate de viteza de deformație. Capacitatea de deformație a PVA-FRCC sub acțiunea încărcărilor dinamice este îmbunătățită prin creşterea raportului apă/liant. De asemenea capacitatea de absorbție a energiei este influențată de raportul apă/liant. Cu cât acest raport creşte capacitatea de absorbție a energiei, a PVA-FRCC este diminuată.

Keywords: *water binder ratio; PVA-FRCC; dynamic mechanical properties; SHPB*

1. Introduction

Cement-based materials are quasi-brittle construction materials characterized by high compressive strength but very low tensile strength, which limits its engineering applications, especially on the dynamic load conditions. It is very important to improve the toughness of cement-based materials employing different methods. Adding fibers, such as steel fiber, polymer fiber and basalt fiber, etc, is a normal method accepted. Another way is adding mineral admixtures such as fly ash, slag or rubbers [1]. The previous researches indicate that the increase of the fiber content and water binder ratio led to the increase of the toughness of fiber reinforced concrete [2]; the addition of the mineral materials can improve the toughness and flexural strength of fiber reinforced concrete [3-4]. Fiber reinforced cement-based composites have excellent crack-resistance capacity and toughness, which allows them to withstand the dynamic loads. Increasing with fiber content, the single and multiple impact resistance capacity are enhanced; the impact toughness is improved [5-8]. Engineered cementitious composite is a unique high performance PVA fiber reinforced cement-based composite (PVA-FRCC) featuring high ductility and strain hardening [9, 10]. The ultra-high ductility is achieved by optimizing the microstructure of the composite employing micromechanical models [11]. PVA-FRCC possesses ultra-high ductility, which gives it advantage in structural seismic resistance, impact resistance and fatigue resistance. In the previous researches, most of the research works focus on theoretical design, mechanical properties, durability and engineering application of PVA-FRCC. There are rare studies on the dynamic properties of PVA-FRCC, especially on the high velocity impact response of PVA-FRCC materials. In this study, high fly ash replacement level of 70% and three water binder ratios of 0.25, 0.32 and 0.40 are selected. The quasi-static compressive strength is conducted to evaluate the quasi-static properties. The dynamic compressive test is conducted by SHPB to study the dynamic response of PVA-FRCC.

* Autor corespondent/Corresponding author,
Tel.: +86-451-86281118, e-mail: rainczt@yahoo.cn

2. Materials and methods

2.1. Raw materials and mixtures design

The mixture design of PVA-FRCC can be found in Table 1. Previous research [12] indicates that the use of higher fly ash content is beneficial for strain hardening behavior, and therefore the higher fly ash content of 70% is used in this research. P.O42.5 ordinary Portland cement (C) is used in all mixtures. The fly ash (FA) is an ASTM Class F fly ash and the physical properties and chemical compositions of the fly ash are listed in Table 2. Silica sand (SS) with fine modulus of 1.03 is adopted in PVA-FRCC mixtures. The specific PVA fibers (F) used in this study are coated with oiling agent that reduces the hydrophilicity of the fiber surface. The mechanical and geometrical properties of the fibers are listed in Table 3. The fiber volume fraction in composite is 2%. Water binder ratio is one of important factors for mixture design. Low water binder ratio is good for obtaining higher strength but is not beneficial for excellent workability of mortar, resulting in fibers balling effect for fiber reinforced cement-based materials. Therefore, three water binder ratio levels (expanded low water binder ratio of 0.25, medium water binder ratio of 0.32 and higher water binder ratio of 0.40) were selected in this research. The high range water reducing admixture (HRWRA) is used to adjust the workability.

2.2. Mixing and specimens preparation

The specimen preparation has an important effect on the mechanical properties of PVA-FRCC, so the following mixing steps are performed: The dry components (including fine silica sand, cement and fly ash) are mixed for 1-2 minutes. Then the water with superplasticizer is added and mixed until the good fluidity and uniformity of mortar is achieved, the mixing time is about 4-5 minutes. Subsequently the fibers are added gradually during mixing, the continuous mixing sustained 6-8 minutes until the fresh PVA-FRCC can reach good consistency and the fibers are uniformly distributed and no balling effect is observed. The mixed fresh composites are cast into different size molds. The specimens are demolded after 24h to secure a hardened state. After demolding, the specimens are cured for 27 days in a standard curing room where the temperature and the relative humidity (RH) are 20±1℃ and 95±2%, relatively. The specimen size for compressive test is 40×40×160 mm and Φ36.5×20 mm for dynamic compressive test.

2.3. Experimental system

The quasi-static compressive test, in accordance with BS EN 196-1[13], is conducted on the specimens using a WDW-100D electronic universal testing machine at a constant strain rate 10-5s^{-1}. The quasi-static compressive strength

Table 1

Mix preparation and quasi-static compressive strength of PVA-FRCCs
Compozițiile utilizate şi valorile rezistențelor quasi-statice la compresiune ale PVA-FRCC

Index	Water *Apă* (kg/m^3)	C (kg/m^3)	FA (kg/m^3)	SS (kg/m^3)	F(kg/m^3)	HRWRA (kg/m^3)	Compressive strength *Rezistența la compresiune* (MPa)
1	326	368	858	446	26	5.7	43.5
2	392	368	858	446	26	3.6	36.5
3	490	368	858	446	26	2.1	20.0

Table 2

Physical properties and chemical compositions of fly ash / *Proprietățile fizice şi compoziția chimică a cenuşilor*

Physical properties / *Proprietăți fizice*		Chemical compositions/ *Compoziția chimică*, %	
Loss on ignition (%) *Pierderea la calcinare*	3.03	SiO_2	65.70
Water required of control (%) *Apa necesară*	95.0	Al_2O_3	20.63
Average grain size (μm) *Dimensiunea medie a particulelor*	3.4	Fe_2O_3	4.65
Density / *Densitatea* (g/cm^3)	2.43	CaO	2.93
Specific surface area (m^2/kg) *Suprafața specifică*	655	MgO	2.25
Strength activity index at 28 days (%) *Indicele de activitate la 28 zile*	79.1	SO_3	0.28

Table 3

Mechanical and geometrical properties of PVA fiber / *Proprietățile mecanice şi geometrice ale fibrelor de PVA*

Length *Lungime* (mm)	Length-Diameter Ratio *Raportul lungime-diametru*	Young's modulus *Modulul lui Young* (GPa)	Elongation *Elongația* (%)	Tensile strength *Rezistența la întindere* (MPa)	Density *Densitatea* (g/cm^3)
8	200	42	7	1600	1.3

decreases obviously with the increase of water binder ratio (Table 1). The strength decreases from 43.5 MPa to 20MPa with the increase of the water binder ratio from 0.25 to 0.40. When the water binder ratio was 0.32, the quasi-static compressive strength can reach 36.5 MPa which can meet the general engineer requirement of structures. The quasi-static compressive strength is recorded to compare with the dynamic compressive strength and further establish a constitutive model to describe the strain rate effect on the dynamic increase factor of PVA-FRCC. A 40-mm-diameter split Hopkinson presser bar (SHPB) system (Fig.1) is used to determine the mechanical properties of PVA-FRCC under dynamic loading.

A short specimen is sandwiched between the incident and transmission bars. Silicon grease is applied on the interfaces between the specimen and the bars to minimize the effect of friction. Attaining constant strain-rate during dynamic loading was a critical problem for cement-based composites. So the pulse shaping technique was applied by sticking a lead sheet on the end face of input bar to achieve the stress equilibrium in the experiment.

We must emphasize that SHPB test principle is based on the one-dimensional elastic wave theory, with two basic assumptions [14]: (a) the incident and transmission bars remain elastic after impact; (b) the state of stress and strain along the specimen can be uniform during impact loading.

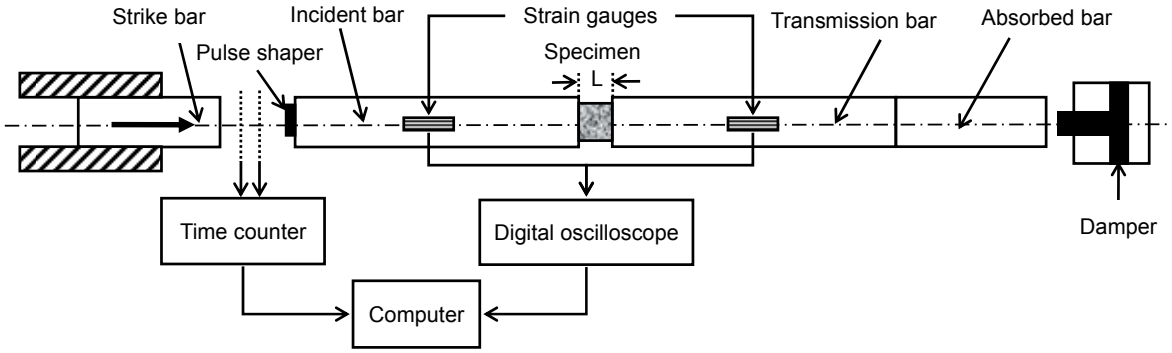

Fig.1 - Sketch of SHPB system / *Schema sistemului SHBP*.

a) W/CM=0.25

b) W/CM=0.32

c) W/CM=0.40

Fig.2 - Failure pattern of PVA-FRCC after SHPB test / *Modalități de cedare a PVA-FRCC după testul SHPB.*

Furthermore, no frictional or dynamic effects are taken into account. The impact of the strike bar on the incident bar results in a compressive incident pulse ε_I. At the interface between incident bar and specimen, part of the pulse is reflected as a reflection pulse ε_R and the rest of the incident pulse is transmitted as a transmission pulse ε_T. The time-dependent strains are calculated from voltage signals, which measured by strain gauges. According to the above assumption (b), we have

$$\varepsilon_I + \varepsilon_R = \varepsilon_T \quad \text{or} \quad \sigma_I + \sigma_R = \sigma_T \tag{1}$$

Where σ_I, σ_R and σ_T (or ε_I, ε_R and ε_T) are the incident, reflected and transmission stress (or strain) propagating within Hopkinson pressure bars, respectively. Thus, the dynamic average strain rate $\dot{\varepsilon}(t)$, strain $\varepsilon(t)$ and stress $\sigma(t)$ of the short specimen can be determined by the measured ε_R and ε_T. The resulting stress and strain of the specimen can be expressed as Eqs. (2)-(4):

$$\dot{\varepsilon}(t) = -\frac{2C_0}{L_S}\varepsilon_R \tag{2}$$

$$\varepsilon(t) = -\frac{2C_0}{L_S}\int_0^t \varepsilon_R dt \tag{3}$$

$$\sigma(t) = E_0 \frac{A_0}{A_S}\varepsilon_T(t) \tag{4}$$

Where, E_0, C_0 and A_0 are the Young's modulus, the elastic wave velocity and the cross-sectional area of the incident (or transmission) bar, respectively; A_S and L_S are the cross-sectional area and the thickness of the specimen.

3. Results and discussion

3.1. *Failure pattern of PVA-FRCC*

The SHPB experiments are conducted at three strain rate levels: 130~140,170~190 and 230~250s^{-1}. As shown in Figure 2, the strain rate has great effect on the failure pattern of PVA-FRCC. Under the strain rate of 130~140s^{-1}, the specimens with different water binder ratio remain almost intact. Only several cracks are observed in specimen a) and b); the edge of specimen c) is damaged more seriously than specimen a) and b). The central through cracks and edge through cracks in PVA-FRCC specimens are observed at the strain rate of 170~190s^{-1}, but the specimens are not crashed probably due to fiber bridge effect. The specimens are broke into distinct fragments under strain rate of 230~250s^{-1} and the number of fragments decreases with the increase of water binder ratio.

3.2. *Dynamic stress-strain relationship of PVA-FRCC*

The dynamic stress-strain curves of PVA-FRCC with different water binder ratio at different strain rate are shown in Figure 3. To facilitate the comparison between the test results for different PVA-FRCC mixtures, the same scales for both axes were used in this figure. The dynamic elastic modulus of PVA-FRCC changes slightly with the increase of strain rate. The slope of curves reduces with the increment of water binder ratio, which means the dynamic elastic modulus decreased.

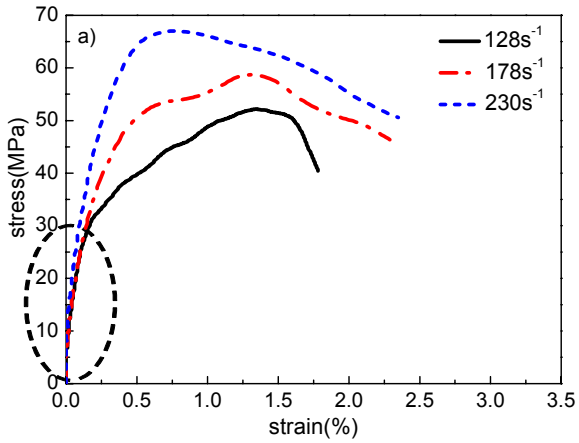

a

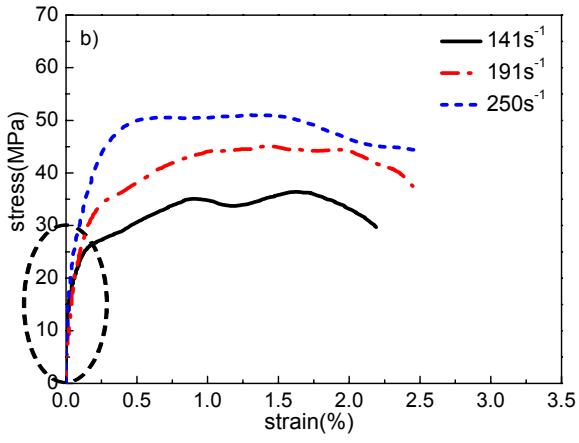

b

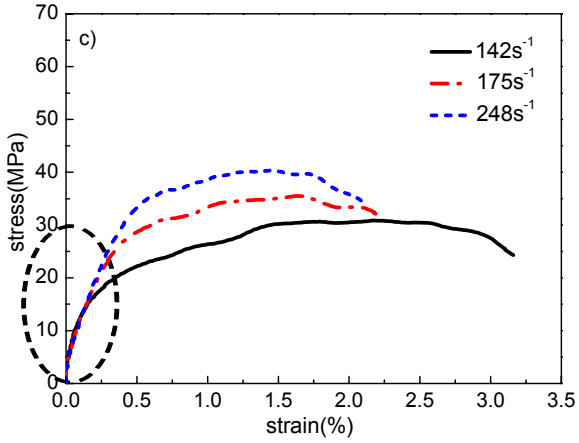

c

Fig.3 - Dynamic stress-strain curves of PVA-FRCC with different water binder ratio / *Curbele efort unitary - deformație specifică la solicitări dinamice pentru PVA-FRCC având diferite rapoarte apă liant:*
a) W/CM=0.25; b) W/CM=0.32; c) W/CM=0.40

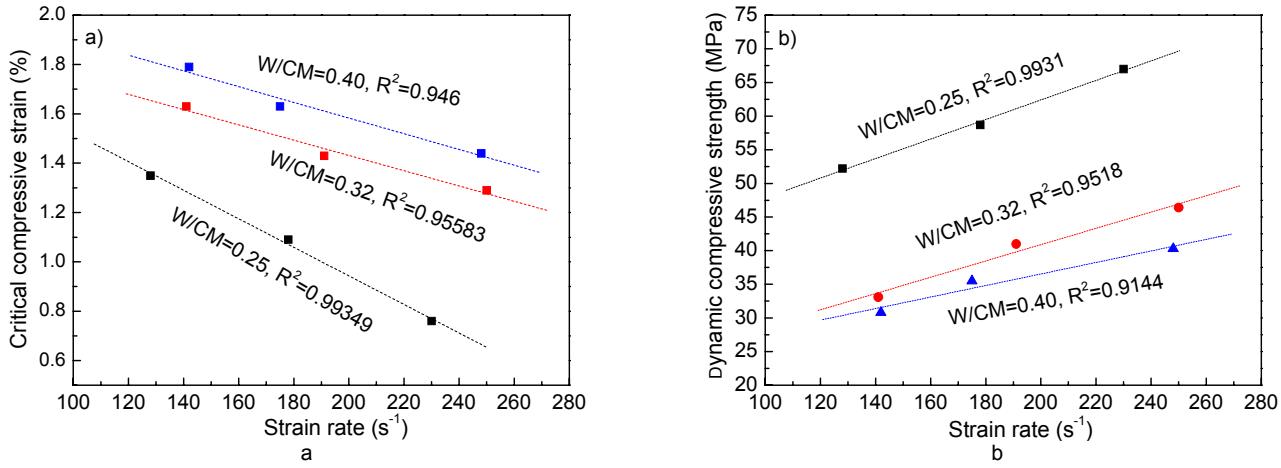

Fig.4 - Critical compressive strain and dynamic compressive strength of PVA-FRCC versus strain rate / *Deformația specifică critică la compresiune şi rezistența la compresiune a PVA-FRCC la solicitări dinamice versus viteaza de deformație.*

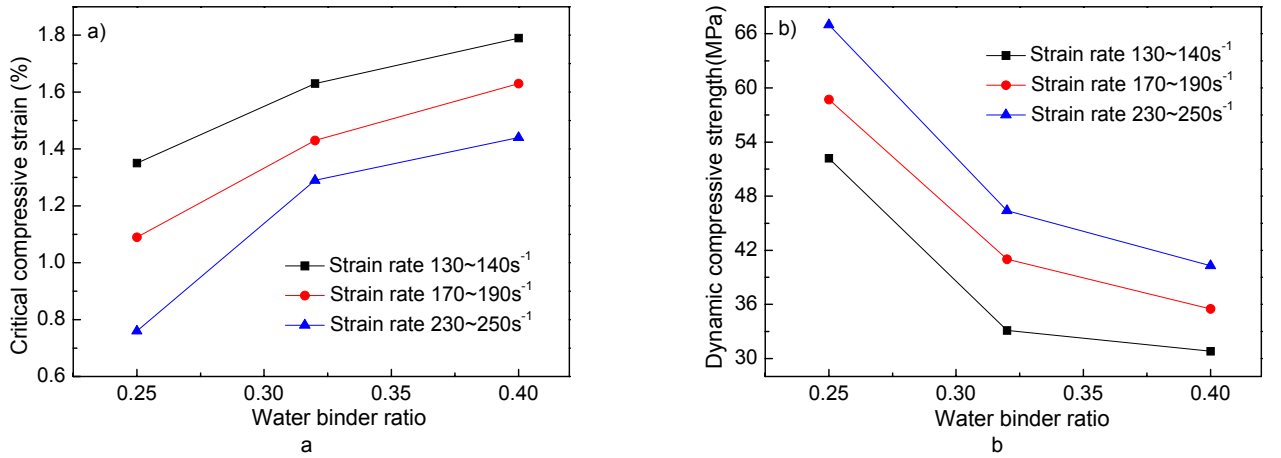

Fig.5 - Critical compressive strain and dynamic compressive strength of PVA-FRCC versus water binder ratio / *Deformația specifică critică la compresiune şi rezistența la compresiune a PVA-FRCC la solicitări dinamice versus raportul apă/liant.*

The PVA-FRCC with 0.25 water binder ratio (Fig.3a) shows a relatively rapid stress reduction after reaching the dynamic peak value, but the PVA-FRCC with 0.32 and 0.40 water binder ratio (Fig.3b and c) shows a gradual stress reduction beyond peak value. Furthermore, PVA-FRCC with different water binder ratio performs dynamic compressive strain hardening behaviour. The critical compressive strain is defined as the strain when the stress reaches its peak value. As shown in Figure 4, the dynamic compressive strength of PVA-FRCC is magnified with the increase in strain rate, but the critical compressive strain of PVA-FRCC decreases with the increase in strain rate.

As shown in Figure 5a, the critical compressive strain increases with the increment of water binder ratio at all three strain rate levels. When the strain rate is 130~140s^{-1}, the PVA-FRCC performed better than the other two strain rate levels on critical compressive strain. The critical compressive strain of PVA-FRCC under strain rate 130~140s^{-1} has a similar trend with the strain rate 107~190s^{-1} along with the increment of water binder ratio, but the critical compressive strain under the strain rate 230~250s^{-1} increases sharply when the water binder ratio increases from 0.25 to 0.32. In addition, the dynamic compressive strength of PVA-FRCC decreases with the increment of water binder ratio at different strain rates. The dynamic compressive strength decreases sharply as the water binder ratio increases from 0.25 to 0.32 and the trend becomes smooth at further increasing water binder ratio to 0.40. The increment of critical compressive strain and the decrease of dynamic compressive strength with the increase of water binder ratio are mainly attributed to the cementitious matrix ductility and interaction of fibers and matrix. The content of excess water in cement paste increases with the increase of the water binder ratio. The evaporation of excess water results in the formation of internal voids and capillary channels in the matrix, and eventually reduces the quality of PVA-FRCC. Otherwise, the ductility of PVA-FRCC is improved with the increase of water binder ratio, the localized tensile properties is improved resulting in the increment of critical compressive strain.

3.3 Strain rate effect

According to the results of quasi-static compression test on the PVA-FRCC, the dynamic increase factor (DIF) [15, 16] can be obtained to illustrate the strain rate effect of PVA-FRCC, which is defined as Eq. (5),

$$DIF = \frac{f_{cd}}{f_{cq}} \quad (5)$$

Where, f_{cd} is the maximum dynamic compressive strength during dynamic compression and f_{cq} is the quasi-static compressive strength of PVA-FRCC.

The DIF of PVA-FRCC with different water binder ratio depends on the logarithm of the strain rate directly, as shown in Figure 6. For the given strain rate, the rate dependence of DIF of PVA-FRCC may be estimated from the following constitutive model:

$$\begin{cases} DIF = 0.03\log\dot{\varepsilon} + 1.14 & \text{for } 10^{-5} \le \dot{\varepsilon} \le 128s^{-1} \\ DIF = 1.88\log\dot{\varepsilon} - 2.69 & \text{for } 128 \le \dot{\varepsilon} \le 250s^{-1} \end{cases} \quad (6)$$

Where, $\dot{\varepsilon}$ is the average strain rate. The transition point from low strain rate sensitivity to high strain rate sensitivity occurs at $128s^{-1}$. After the inflection point, a steep increase in DIF is observed until $250s^{-1}$, which exhibits high sensitivity to the strain rate. The model for estimating strain rate effect of PVA-FRCC is similar to results reported by some researchers [16-18]. However, different equations have been derived for the dynamic mechanical properties of different concrete-like materials.

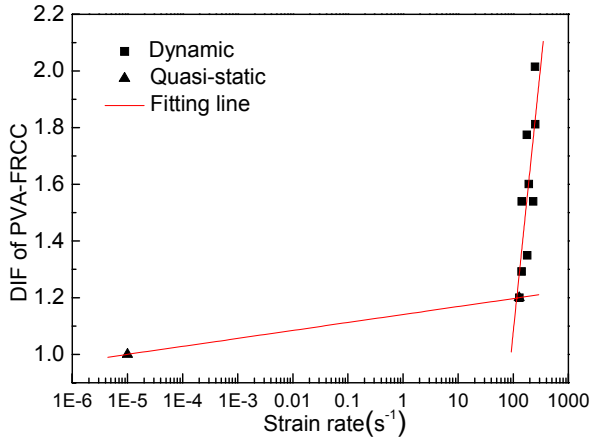

Fig.6 - Dynamic increase factor of PVA-FRCC versus strain rate / *Factorul de creştere dinamic a PVA-FRCC versus viteza de deformație.*

3.4 Energy absorption effect

The energy dissipation by sample was divided into strain energy from sample deformation, interface energy from new cracks formation and fraction energy from contact between sample and bars, etc. The energy dissipation can calculate from input energy W_I, reflection energy W_R and transmission energy W_T according to Eqs. (7)-(9) [19]:

$$W_I = \frac{A_0C_0}{E}\int\sigma_I^2dt = A_0EC_0\int\varepsilon_I^2dt \quad (7)$$

$$W_R = \frac{A_0C_0}{E}\int\sigma_R^2dt = A_0EC_0\int\varepsilon_R^2dt \quad (8)$$

$$W_T = \frac{A_0C_0}{E}\int\sigma_T^2dt = A_0EC_0\int\varepsilon_T^2dt \quad (9)$$

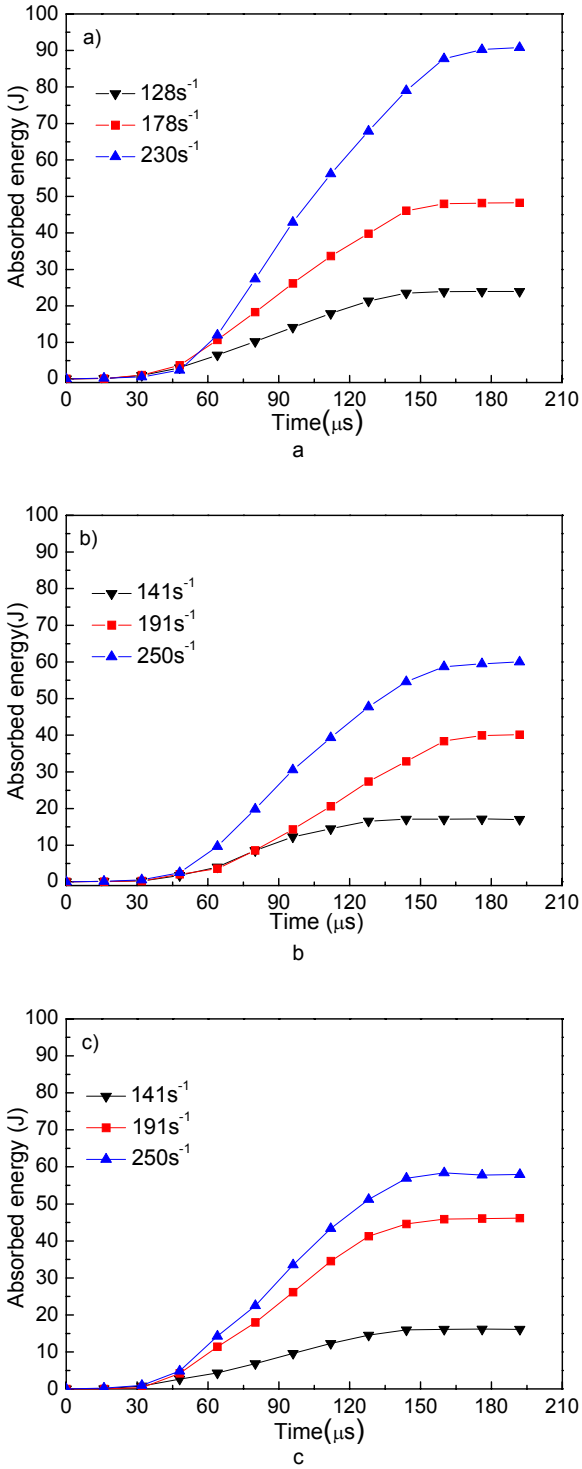

Fig.7 - Absorbed energy of PVA-FRCC versus time
Energia absorbită a PVA-FRCC versus timp.

Where σ_I , σ_R and σ_T are the stress corresponding to input wave, reflection wave and transmission wave, respectively. If not considering the energy dissipation by fraction, the absorbed energy by sample can be calculated by Eq. (10):

$$W_L = W_I - (W_R + W_T) = A_0 E C_0 \int (\varepsilon_I^2 - \varepsilon_R^2 - \varepsilon_T^2)\, dt \quad (10)$$

Figure 7 shows the absorbed energy-time curves of PVA-FRCC with different water binder ratio at different strain rates. In this study, the vacuum silica grease was greased on the ends of specimen in order to weaken fraction. In the first 45μs, the energy was mainly dissipated by fraction, so the change in energy absorption is very small. As the time increasing, the elastic and plastic deformation occurred meanwhile the microcracks emerged at the weaknesses. Both of them need dissipated amount of energy, which results in sharply increased of energy. With the increase of deformation and the propagation of cracks, the energy dissipation will further increased. At last, the specimen was absolutely crashed and then the absorbed energy tended to be constant. We can also find that the absorbed energy of PVA-FRCC performed obvious rate dependency. On the one hand, the kinetic energy provided by the SHPB system increases with the increment of strain rate, then the destruction degree of specimen was accelerated which resulted in the increasing of energy dissipation. On the other hand, the chemical bond between fibers and matrix also performed rate dependency which can be another reason why the absorbed energy of PVA-FRCC performed rate dependency [20]. Increasing with the water binder ratio, the energy absorbed capacity was deteriorated. The strength of PVA-FRCC was so low that it could be quickly damaged after suffering high velocity impact. So the interval of reaching constant of absorbed energy decreased with the increase of water binder ratio.

4. Conclusions

Based on the dynamic compression tests conducted on a 40-mm-diameter SHPB system at high strain rates in the range of 128~250s^{-1}, the dynamic mechanical properties of PVA-FRCC are studied and the main conclusions can be drawn from the present study:

(1) The quasi-static compressive strength obviously decreased with the increase of water binder ratio. The strength decreases from 43.5MPa to 20MPa with the increase of water binder ratio from 0.25 to 0.40. The compressive strength was still 36.5 MPa when the water binder ratio was 0.32.

(2) PVA-FRCC can maintain almost intact under the strain rate of 130~140s^{-1}; the specimens are crushed when the strain rate reaches more than 230s^{-1} and the number of fragment decreases with the increase of water binder ratio.

(3) Strain rate effect is one of the most important factors dominating the behaviour of PVA-FRCC under dynamic loading. The critical compressive strain increases and the dynamic compressive strength increases with the increase of strain rate. Additionally, a simple constitutive model is established to describe the strain rate effect on dynamic increase factor of PVA-FRCC, and the transition point from low strain rate sensitivity to high strain rate sensitivity occurs at 128s^{-1}.

(4) The water binder ratio plays an important role on the mechanical properties of PVA-FRCC under dynamic loading. At the same level of strain rate, the dynamic peak stress decreased and the peak strain increased with the increase of water binder ratio. The absorbed energy of PVA-FRCC with different water binder ratio performs rate dependency and the energy absorption capacity of PVA-FRCC is weakened with the increase of water binder ratio.

REFERENCES

1. A.R. Khaloo, M. Dehestani and P. Rahmatabadi, Mechanical properties of concrete containing a high volume of tire–rubber particles, Waste Management, 2008, **28**, 2472.
2. M.C. Nataraja, N. Dhang and A.P. Gupta, Stress-strain curves for steel-fiber reinforced concrete under compression, Cement and Concrete Composites, 1999, **21**, 383.
3. H. Yazıcı, M.Y. Yardımcı, S. Aydın and A.Ş. Karabulut, Mechanical properties of reactive powder concrete containing mineral admixtures under different curing regimes, Construction and Building Materials, 2009, **23**, 1223.
4. J. Ksenija, Ć. Goran, N. Dragan and B. Dragan. Mechanical properties of ultra high performance self compacting concrete with different mineral admixtures, Romanian Journal of Materials, 2011, **41** (3), 211.
5. W. Sun, J. Lai, Dynamic mechanical behavior of ultra-high performance cementitious composites on impact loads, Journal of PLA University of Science and Technology (in Chinese), 2007, **8**(5), 443.
6. C. Jiao, W. Sun, P. Gao, Dynamic mechanical properties of steel-fiber reinforced ultra high strength concrete, Engineering Mechanics (in Chinese), 2006, **23**(8), 86.
7. W. Li, J. Xu, Impact characterization of basalt fiber reinforced geopolymeric concrete using a 100 mm diameter split Hopkinson pressure bar, Materials Science and Engineering A, 2009, **513–514**, 145.
8. Z. Wang, L. Wu and J. Wang, A study of constitutive relation and dynamic failure for SFRCC in compression, Construction and Building Materials, 2010, **24**, 1358.
9. V.C. Li, S.X. Wang and C. Wu, Tensile strain-hardening behavior of polyvinyl alcohol engineered cementitious composite (PVA-ECC), ACI Materials Journal, 2001, 483.
10. V.C. Li, On engineered cementitious composites (ECC): a review of the material and its applications, Journal of Advanced Concrete Technology, 2003, **1**(3), 215.
11. E.H. Yang, V.C. Li, Strain-hardening fiber cement optimization and component tailoring by means of a micromechanical model, Construction and Building Materials, 2010, **24**, 130.
12. E.H. Yang, Y.Z. Yang and V.C. Li, Use of high volumes of fly ash to improve ECC mechanical properties and material greenness, ACI Materials Journal, 2007, 303.
13. BS EN 196-1:2005, Methods of testing cement—Part 1: Determination of strength, British Standard Institute (BSI): 2005.

14. L.L. Wang, Foundation of stress waves (second edition in Chinese), National Defense Industry Press, Beijing, 2010.
15. C.A. Ross, J.W. Tedesco and S.T. Kuennen, Effects of strain-rate on concrete strength, ACI Materials Journal, 1995, **92**(1), 37.
16. C.A. Ross, D.M. Jerome, J.W. Tedesco, and M.L. Hughes, Moisture and strain rate effects on concrete strength, ACI Materials Journal, 1996, **94**, 293.
17. W.M. Li, J.Y. Xu, Mechanical properties of basalt fiber reinforced geopolymeric concrete under impact loading, Materials Science and Engineering A, 2009, **505**, 178.
18. W. Wu, W.D. Zhang and G.W. Ma, Mechanical properties of copper slag reinforced concrete under dynamic compression, Construction and Building Materials, 2010, **24**, 910.
19. Y. Zhai, G. Ma, J. Zhao and C. Hu, Comparison of dynamic capability of granite and concrete under uniaxial impact compressive loading, Chinese Journal of Rock Mechanics and Engineering (in Chinese), 2007, **26** (4), 762.
20. E.H. Yang, V.C. Li, International RILEM workshop on high performance fiber reinforced cementitious composites (HPFRCC) in structural Applications, Honolulu, Hawai'i, May 2005, p. 83.

****

NOUTĂȚI / NEWS

Biomateriale elastomere pentru ingineria de țesut
Elastomeric biomaterials for tissue engineering

Biomaterialele joacă un rol important în ingineria construcției de țesut, lucrând ca o matrice extracelulară artificială care susține regenerarea. Deoarece capacitatea de întindere elestică este o proprietate mecanică majoră a multor tipuri de țesuturi, s-au făcut eforturi pentru dezvoltarea biomaterialelor elastomere folosite în ingineria de țesuturi. Se introduc definițiile biomaterialelor, biocompatibilității şi elasticității în contextul ingineriei de țesut. Urmează o trecere în revistă sistematică a cauciucurilor termoplastice, a elastomerilor reticulați chimic, a proteinelor elastice şi a compozitelor cu umplutură ceramică pe bază de elastomer.

Fiecare secțiune include o descriere detaliată a sintezei chimice a polimerului, importantă pentru înțelegerea proprietăților sale unice, urmată de o discuție despre biocompatibilitatea şi biodegradabilitatea sa, două trăsături esențiale ale biomaterialelor în majoritatea aplicațiilor din ingineria de țesut.

Proprietățile mecanice şi aplicațiile în ingineria de țesut sunt apoi revizuite pentru fiecare polimer, detaliat, identificând subiectele de interes pentru aplicațiile curente şi viitoare din domeniu. În final sunt rezumate realizările majore şi problemele nesoluționate în cazul biomaterialelor elastomere subliniind cei mai importanți candidați până la ora actuală.

Material prelucrat de / *Material worked by* Alina Melinescu
Sursa / *Source* : Progress in Polymer Science xxx (2012)

Biomaterials play a critical role in engineering of tissue constructs, working as an artificial extracellular matrix to support regeneration. Because the elastic stretchability is a major mechanical property of many tissue types, huge efforts have been invested into the development of elastomeric biomaterials that mimic that of native tissue. Indeed, for the repair of most soft tissue types, one of the major problems encountered by biomaterials scientists has been difficulty in simply replicating this complex elasticity. This article provides a comprehensive review on the elastomeric biomaterials used in tissue engineering. Definitions of biomaterials, biocompatibility and elasticity in the context of tissue engineering are introduced. This is followed by systematic review of thermoplastic rubbers, chemically crosslinked elastomers, elastic proteins and elastomer-based ceramic-filled composites. Each section includes a detailed description of the chemical synthesis of the polymer critical to understanding of its unique properties, followed by discussion of its biocompatibility and biodegradability, two essential features of biomaterials in most tissue engineering applications. The mechanical properties and applications in tissue engineering are then reviewed for each polymer in great detail, with identification of specific challenges for its current and ongoing application in the field. Finally, the major achievements and remaining challenges for elastomeric biomaterials are summarized, with emphasis on the most important candidates to date.

****